International Journal of Science and Research (IJSR)
ISSN (Online): 2319-7064
Index Copernicus Value (2013): 6.14 | Impact Factor (2015): 6.391

Non-Hillock Formation and Population of Ag/TiO_2 Nanoparticles through Stepwise Annealing

Patrick D. Nsimama

Department of Science and Laboratory Technology, Dar Es Salaam Institute of Technology
P. O. Box 2958, Dar Es Salaam, Tanzania

Abstract: ***Magnetron sputtered Ag nanofilms were coated on TiO_2 layers deposited on SiO_2/Si substrates. The films were then post-annealed to a maximum temperature of 500 ^{0}C at different time and temperature intervals according to the chosen number of annealing steps to produce non-hillock dewetted Ag nanoparticles. The annealing steps ranged from one to four. The cumulative annealing time was fixed at 30 minutes. The changes of particle distribution, morphological and structural properties of the non-hillock dewetted particles with the number of annealing steps were investigated. Scanning electron microscope (SEM) and X-ray Diffraction (XRD) machine were employed for the films morphological and structural analysis respectively. The population of the dewetted particles increased with the increase in the number of annealing steps. However, the dewetted areas and particle sizes decreased with the increase in the number of annealing steps. Higher densities of dewetted particles on the nanoscale were only possible at higher numbers of annealing steps. The highest circularity of the dewetted particles was recorded by the sample that was annealed in two equal steps. There wasn't any significant difference among the particle crystal structures of films annealed at different steps. The XRD patterns were mainly from metallic Ag for films annealed at higher number of steps. The sample annealed in one step had XRD peaks from both Ag and TiO_2.***

Keywords: Ag/TiO_2, hillock, stepwise-annealing, dewetting, nanoparticle

1. Introduction

Tuning the catalyst particle size has been established as one of the most promising approaches to tailor its functional properties for catalytical applications [1]. Consequently, the preparation of uniformly sized catalytic nanoparticles is now considered as the most important step toward best performance of catalysts. Among mostly common metals for catalytical applications is Ag as evidenced by a number of published works [2]-[5]. Dewetting of Ag thin films on oxide substrates through thermal annealing in different atmospheres stands as the versatile, low cost and fast technique for producing nanoparticles. However, the production of uniform Ag nanoparticles has always been reported to be an uphill task due to the hillock formation of the Ag particles.

Hillock formation in Ag thin films during annealing has been reported by many researchers [2], [3], [6], [7]. The term "hillock" is always referred to elevated individual grains, which protrude substantially above the average thickness of polycrystalline thin film [8]**.** Various mechanisms, including interfacial diffusion, surface diffusion and grain boundary diffusion have been proposed for hillock growth in the metal films. Essentially, hillocks are formed by mass transportation along grain boundaries and surfaces driven by the relaxation of compressive stress [6]. The formation of hillocks has been taking place irrespective of the annealing atmospheres. The hillock morphologies have been reported to remain unchanged even after annealing for many hours [3]. Compressive stresses, which are the main cause of hillock formation, have been reported to be originating from the big difference of the thermal coefficient of expansions of the Ag films with the substrates [3]. One of the common substrates for Ag depositions is silicon (Si) whose thermal coefficient expansion is 3 x 10^{-6} m/mK, far less than that of Ag thermal coefficient expansion (18 x 10^{-6} m/mK) [3]. To minimize, the compressive stress and produce particles with useful morphological applications, such as in catalysts, Ag ought to be deposited on a layer with higher thermal coefficient of expansion. TiO_2 layer is a potential candidate due to the fact that its thermal coefficient of expansion (9 x 10^{-6} m/mK) is about three times that of Si, which reduces to a great extent the thermal expansion difference with Ag. However, there is little literature addressing on this problem. The tuning of particle sizes and shapes through annealing sequences hasn't been reported in literature to the best of my knowledge

In the current work we report on the formation and population of dewetted non-hillock Ag nanoparticles through stepwise annealing in argon atmosphere at a maximum temperature of 500 ^{o}C for a cumulative time of 30 minutes. We attribute the achievement to the favourable thermal conditions resulting from stepwise annealing and the inclusion of TiO_2. Production of populated non-hillock formation is crucial for catalytical applications.

2. Materials and Methods

The chamber of the sputtering machine (*LA440S Von Ardenne Enlargentechnik GMBH)* was evacuated to a base pressure of 2 x 10^{-7} mbar before introducing the argon gas at 80 sccm flow rate. The RF power was fixed at 200 W. Then a 100 nm pure TiO_2 was deposited using RF sputtering on a 100 nm SiO_2/Si substrate. The substrate size was 15 x 15 mm^2. Subsequently, a 30 nm metallic Ag target (purity 99.9999 %) was sputtered using the DC mode. The deposited Ag/TiO_2 nanofilms were then annealed using the thermal annealing system (*Eurotherm-Nabertherm*) in argon atmosphere, for a cummulative time of 30 minutes per sample at a fixed maximum temperature of 500^o C stepwise in steps ranging from one to four as detailed in Table 1.

Licensed Under Creative Commons Attribution CC BY

Table 1: The detailed annealing sequences for Ag/TiO_2 samples

Sample	*No. of steps*	*Temperature/Time*			
(a)	One	500 °C/30 mins			
(b)	Two	250 °C/15 mins		500 °C/15 mins	
(c)	Four (A)	125°C/ 7.5 mins.	250°C/ 7.5 mins	375°C/ 7.5 mins	500°C/ 7.5 mins
(d)	Four (B)	300 °C/ 15 mins.	366 °C/ 5 mins	433 °C/ 5 mins	500°C/ 7.5 mins
(e)	Four (C)	100°C/ 5 mins.	200 °C/ 5 mins	300 °C/ 5 mins	500 °C/ 15 mins

The argon flow rate during annealing was fixed at 20 sccm. Prior to annealing, the chamber was purged with argon at a flow rate of 40 sccm for one hour. The film morphologies were investigated by a high-resolution scanning electron microscopy (*SEM, Hitachi S-4800*) in which the SEM images were recorded using mixed signals from secondary electrons (SE) and back scattered electrons (BSE), in order to get the images with both high contrast and high resolution. The *SIEMENS D 5000* theta-theta diffractometer machine with Cu Kα radiation of λ = 1.5405 nm was employed for the Bragg Brentano X-ray diffraction (BBXRD) data collection. The *ImageJ* free software was used to analyze the distribution of the dewetted particles.

3. Results and Discussion

3.1 SEM Results

Figure 1 shows the 5 µm x 5 µm scale SEM images for the magnetron sputtered Ag/TiO_2 samples annealed at different number of steps at a fixed maximum temperature of 500° C for a total time of 30 minutes as detailed in Table 1. The in-set SEM images are the higher magnification images for the respective images. It is clear from the results that the density of dewetted particles was increasing with the increase of the annealing steps.

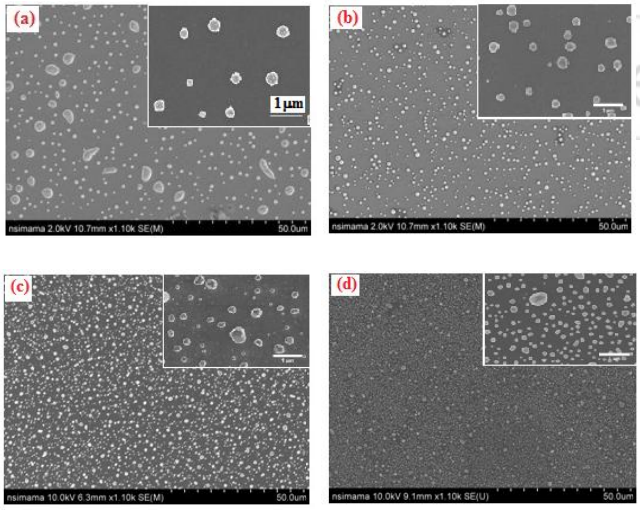

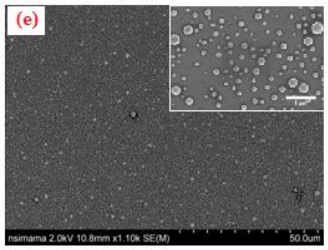

Figure 1: SEM images for Ag/TiO_2 nanofilms annealed at 500 °C stepwise in (a) One step (b) Two equal steps (c) Four steps (A) (d) Four steps (B) (e) Four steps (C) [details in Table 1].

It is interesting to see that the samples, which were annealed in special sequences, i.e., four steps (B) and four steps (C) resulted into higher densities than the sample annealed in four equal steps (four steps (A)). The implication is that short durations of annealing have a positive sequence to the density of the dewetted particles. There is also a decrease in particle sizes as observed from the SEM images with the increase in the number of annealing steps. The larger particles in the film annealed in one step is possibly due to the coalescence of small particles, which merge to form one larger nanoparticle. The driving force of this phenomenon is simply the natural tendency to reduce the total interfacial energy of the system. During particle coalescence, entire nanoparticles can migrate on the substrate surface and coalesce if motion yields overall system-energy reduction resulting into a size distribution that is usually skewed toward larger particles [9].

3.2 Particle distribution analysis

In the particle distribution analysis, the 50 µm x 50 µm SEM images were used instead of 5 µm x 5 µm images. For each sample, SEM images taken from four different positions were taken and the number of dewetted particles and particle surface areas were computed using ImageJ software. The particles were assumed to be spherical in shape. Thereafter, their mean values were calculated and the results are discussed in sections 3.2.1.

3.2.1 The number of dewetted particles and dewetted area

The variation of the average number of dewetted particles and dewetted areas with the number of annealing steps is shown in Figure 2. In general the particles density varies inversely with the dewetted area as expected. This is showing consistency of the results, since the two tend to have a similar dewetting trend as reported elsewhere [10]. The number of dewetted particles increased by a factor of almost 8 from a sample annealed in one step to a sample annealed in four steps (A). This suggests that, increasing the number of annealing steps favours more dewetted particles. The highest population of the dewetted particles was recorded by the sample that was annealed in four steps (C), annealed for 5 minutes at 100 °C, 5 minutes at 200 °C, 5 minutes at 300 °C and 15 minutes at 500 °C. Comparing the samples annealed in four steps (A) and four steps (C), one can notice that the number of dewetted particles increased by a factor of almost 8.

Licensed Under Creative Commons Attribution CC BY

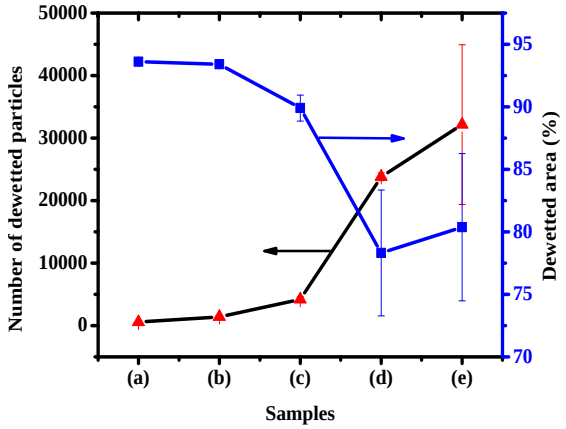

Figure 2: Variation of the number of dewetted particles and dewetted areas with the stepwise annealing of Ag/TiO_2 nanofilms annealed at 500 ^oC (a) One step (b) Two equal steps (c) Four steps (A) (d) Four steps (B) (e) Four steps (C) [details in Table 1].

This indicates that annealing for short intervals of time at the initial stages and thereafter for longer times at the final stages has a positive influence on the number of dewetted particles.

Regarding the changes of dewetted areas with the annealing steps, the dewetted areas (in percentage) are generally high (above 75 %) with the exception of samples (d) and (e), which have very low percentages of dewetted areas. This is due to the large numbers of dewetted particles from the two samples, which occupy more space.

3.2.2 Particle size and uniformity

The variation of the average particle sizes with the samples is shown in Figure 3.

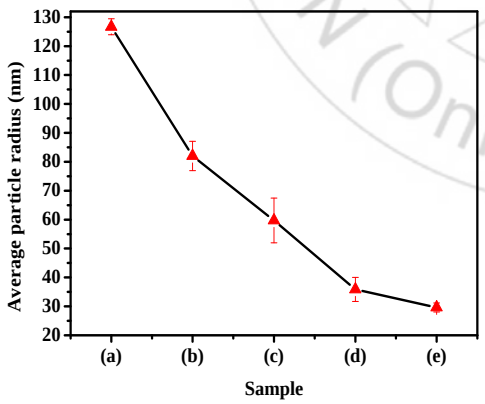

Figure 3: The variation of average particle size with the annealing steps for Ag/TiO_2 nanofilms annealed at 500 ^oC (a) One step (b) Two equal steps (c) Four steps (A) (d) Four steps (B) (e) Four steps (C) [details in Table 1

There is a decrease in the average particle sizes with the increase in the number of annealing steps down to 29.6 nm of sample (e) from 126.7 nm of sample (a). Short intervals of annealing times and temperatures seem to be favouring merging of small particles, a situation which is always observed during prolonged annealing. It is likely that at higher numbers of annealing steps the dewetting process is dominated by Ostwald ripening, in which the particles are not in contact and the reduction of surface energy drives the mass transport. Both nanoparticles exchange atoms resulting into smaller nanoparticles losing atoms and thereby becoming smaller while the large ones gain atoms and thus become even bigger. Generally, Ostwald ripening results in a size distribution that is usually skewed toward smaller particles [9].

The uniformity in terms of particle sizes for this case is reflected by the heights of the error bars. It is evident from the figure that the particle size uniformity generally increases with the increase in the number of annealing steps, with the best uniformity being recorded by sample (e). The average particle radius of sample (e), which is 29.6 nm is almost equal to the original film thickness of Ag, i.e., 30 nm. This reflects that the film consists of columnar grains of uniform morphology as has always been the case [10]. A further particles distribution analysis is presented in Table 2 in which a comparison of the number of particles in three different size zones is presented. The results are from the representative SEM images for the samples.

Table 2: Particle distribution summary according to their sizes in three different zones from 50 um x 50 um representative SEM images

	Particle surface area/particle size range			
Sample	$0 < A \leq 0.0315$ (sq. µm) $0 < r \leq 50$ (nm)	$0.0315 < A \leq 0.1256$ (sq. µm) $50 < r \leq 100$ (nm)	$A > 0.1256$ (sq. µm) $r > 100$ (nm)	Total number of particles
(a)	41	193	309	543
(b)	440	517	413	1370
(c)	1702	1550	535	3787
(d)	21741	2780	79	24600
(e)	27133	1651	225	29009

The graphical analysis per sample of the number of particles in each range in Table 2 is as shown in Figure 4, where the vertical summation for each sample sums to 100 %. The results show that sample (a) has the highest percentage of particles with radii greater than 100 nm. It has also above 35 % of particles in the size zone 50-100 nm. However, it has the lowest percentage of the 0-50 nm particle sizes. Sample (b) has almost balanced percentages ranging approximately from 30- 35 of particle sizes from all three zones. So, annealing two times leads to almost equal percentages of particles from all of the three zones. Annealing in four equal steps (sample (c)), lead to almost equal percentages of particles in the 0-50 nm and 50-100 nm zones. The two zones make more than 85 % of the total number ofparticles in sample (c). On the other hand, both samples (d) and (e) are dominated by the 0-50 nm zone particle sizes representing more than 90 % of the total number of particles. Particles falling on other zones represent only a small percentage.

Licensed Under Creative Commons Attribution CC BY

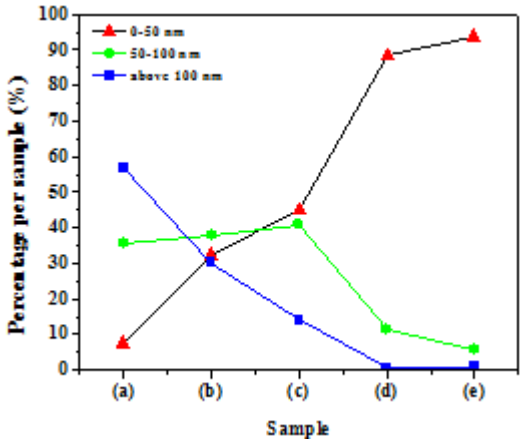

Figure 4: Percentage analysis of particle sizes per sample for the three zones as per Table 2 for the Ag/TiO_2 nanofilms annealed at 500 °C stepwise (a) One step (b) Two equal steps (c) Four steps (A) (d) Four steps (B) (e) Four steps (C) [details in Table 1]

It can therefore be concluded that achievement of highest percentages of nanoparticles in the dewetting process of Ag/TiO_2 is only possible when higher numbers of annealing steps are applied.

The changes of particle circularities with the number of annealing steps were also studied.

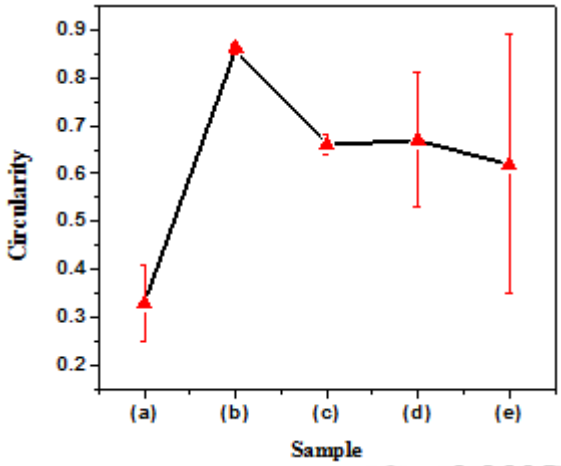

Figure 5: The changes of the particle circularity of the dewetted particles with the number of annealing steps for the Ag/TiO_2 nanofilms annealed at 500 °C stepwise (a) One step (b) Two equal steps (c) Four steps (A) (d) Four steps (B) (e) Four steps (C) [details in Table 1]

Circularity, which is a measure of how spherical are the particles, has two extreme numbers 1 and 0 representing a perfect circle and an elongated polygon respectively. The result is as shown in Figure 5. It can be observed from the results that highest circularity is recorded by the sample that was annealed in two steps. The lowest circularity is coming from the sample that was annealed in only one step. Annealing in four steps gives comparable values of the circularity, but less than the sample annealed in two steps.

3.3 XRD Results

The BBXRD patterns for the Ag/TiO_2 samples annealed at different number of annealing steps are shown in Figure 6.

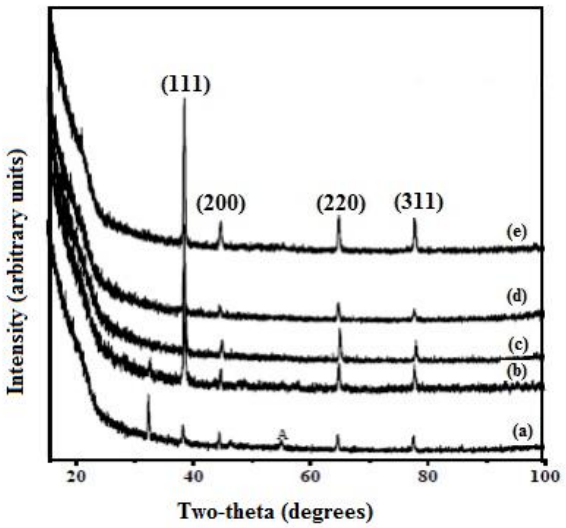

Figure 6: BBXRD patterns for Ag/TiO_2 nanofilms annealed at 500 °C stepwise (a) One step (b) Two equal steps (c) Four equal steps (A) (d) Four steps (B) (e) Four steps (C) [details in Table 1

All the samples are characterized by the highest intensity from the reflection of (111) orientation at 2θ = 38.09° coming from metallic Ag [11]. Additionally, they displayed XRD patterns with common metallic Ag peaks at 2θ = 44.23° and 81.56° with orientations (200) and (222) respectively [12]. The peak at around 33° observed in samples annealed in one and two steps is possibly coming from the substrate (Si (100)) [13]. The sample annealed in only one step has an anatase peak at 2θ = 55.6° (**JCPDS 78-2486**). It is likely that Ag underwent diffusion into TiO_2 during the annealing process as the heating process was constant and continuous for 30 minutes. Diffusion of Au into TiO_2 was reported elsewhere [13] when annealing was done at 400 °C. There is no such a peak to samples annealed in more than one step, presumably implying that stepwise annealing in higher number of steps reduces the diffusion of metallic Ag into TiO_2.

4. Conclusion

Ag/TiO_2 nanofilms were successfully prepared by magnetron sputtering and annealed stepwise to obtain non-hillock dewetted Ag particles in argon atmosphere for a fixed maximum temperature of 500 °C and cumulative time of 30 minutes. The number of annealing steps has a profound influence on the population and size of the dewetted particles.

The population of the dewetted particles increased with the increase in the number of annealing steps. However, the dewetted areas and particle sizes decreased with the increase in the number of annealing steps. Higher densities of particles on the nanoscale were only possible at higher numbers of annealing steps. The highest circularity of the dewetted particles was recorded by the sample that was annealed in two equal steps. There wasn't any significant difference among the particle crystal structures of films annealed at different steps. The XRD patterns for films annealed for more than one step were mainly from metallic

Licensed Under Creative Commons Attribution CC BY

Ag. However, the film that was annealed in one step only had the anatase peak too.

5. Acknowledgements

This work was funded by the Alexander von Humboldt Foundation, Bonn, Germany with a fellowship of my stay in Ilmenau. It was partly funded by the Deutsche Forschungsgemeinschaft (DFG grant Scha 632/20).

The author would like to acknowledge Prof. Peter Schaaf, Dr. Dong Wang and Mr. Andreas Herz all from TU Ilmenau (Institute of Materials Engineering and Institute of Micro- and Nanotechnologies MacroNano®, Chair Materials for Electrical Engineering and Electronics) for introducing me to the dewetting technique. Joachim Döll and Dr. Rolf Grieseler also from TU Ilmenau are highly acknowledged for their help in the sample preparation.

References

[1] Satoko Kuwano-Nakatani, Takeshi Fujita, Kazuki Uchisawa, Daichi Umetsu, Yu Kase, Yusuke Kowata, Katsuhiko Chiba, Tomoharu Tokunaga, Shigeo Arai, Yuta Yamamoto, Nobuo Tanaka and Mingwei Chen, "Environment-sensitive thermal coarsening of nanoporous gold", (2015), Materials Transactions, **56**, No. 4, 468-472.

[2] S. K. Sharma, S. V. M Rao and N. Kumar, "Hillock formation and agglomeration in silver films prepared by thermal evaporation", Thin Solid Films, (1986), **142**, L95-L98.

[3] S. K. Sharma and J. Spitz, "Hillock formation, hole growth and agglomeration in thin silver films", Thin Solid Films, (1980), **65**, 339-350.

[4] Jongpil Ye, "Investigation of the mechanism of solid-state dewetting of silver thin films using spatial correlation analysis of hole patterns", Appl. Phys. Express, (2014), **7**, 085601.

[5] P. D. Nsimama, "Morphological and structural properties of silver nanofilms annealed by RTP in different atmospheres", American Journal of Nano Research & Applications, (2015), **3**, 99-104.

[6] H. Sun, Z. X. Song, F. Ma, J. M Shan, K. W. Xu, "Microstructure, formation mechanism and compression plasticity of regularly faceted Cu particles", Scripta Materialia, (2009), **60**, 305-308.

[7] Suk J. Kim, Eric A. Stach, Carol A. Handwerker, "Silver layer instability in a SnO2/Ag/SnO2 trilayer on silicon", Thin Solid Films, (2012), **520**, 6189-6195.

[8] O. Kovalenko, J. R. Greer, E. Rabkin, "Solid-state dewetting of thin iron films on sapphire subtrates controlled by grain boundary diffusion", Materialia, (2013), **61**, 3148-3156.

[9] Mikhael Bechelany, Xavier Maeder, Jessica Riesterer, Jihanve Hankache, Damiana Lerose, Silke Christiansen, Johann Michler and Laetitia Philippe, "Synthesis Mechanisms of Organized Gold Nanoparticles: Influence of Annealing Temperature and Atmosphere",Cryst. Growth & Design, (2010), **10**, 587-596.

[10] Claudia Manuela Müller, Ralph Spolenak, "Microstructure evolution during dewetting in thin Au films", Acta Materialia, (2010), **58**, 6035-6045.

[11] Fanming Meng, Zhaoqi Sun, Xueping Song, "Synthesis, characterization, properties and applications of nanosized photocatalytic materials", Journal of Nanomaterials, (2012), Article ID 310514, 7 pages.

[12] X. H Yang, H. T. Fu, K. Wong, X. C Jiang, A. B. Yu, "Hybrid Ag@TiO2 core-shell nanostructures with highly enhanced photocatalytic performance", Nanotechnology, (2013), **24**, 415601 (10 pp).

[13] R. C. Adochite, D. Munteanu, M. Torrell, I. Cunha, E. Alves, N. P. Barradas, A. Cavaleiro, J. P. Riviere, E. Le Bourhis, D. Eyidi, F. Vaz, "The influence of annealing treatments on the properties of Ag:TiO2 nanocomposite films prepared by magnetron sputtering", App. Surf. Mater. (2012), **258**, 4028-4034.

Author Profile

Patrick D. Nsimama received his BSc (with Education) in 1992 at the University of Dar Es Salaam. He got his MSc (Physics) at the same university in 2000 and later in 2001 joined the Dar Es Salaam Institute of Technology as an assistant lecturer at the Department of Science and Laboratory Technology. He joined his PhD program at the University of the Free State, South Africa, in 2008 and graduated in 2011. He thereafter went for a postdoctoral program at Ilmenau Technical University, Germany in 2013, where he stayed for 20 months. His areas of interest are among others, semiconductors, photovoltaics, photoluminescence, bioinformatics and metallic catalysts.

.

Licensed Under Creative Commons Attribution CC BY